Composition of critical clusters in ternary nucleation of water–n-nonane–n-butanol

Y. Viisanen and R. Strey

Citation: The Journal of Chemical Physics **105**, 8293 (1996); doi: 10.1063/1.472683
View online: http://dx.doi.org/10.1063/1.472683
View Table of Contents: http://scitation.aip.org/content/aip/journal/jcp/105/18?ver=pdfcov
Published by the AIP Publishing

Composition of critical clusters in ternary nucleation of water–*n*-nonane–*n*-butanol

Y. Viisanen[a] and R. Strey[b]
Max-Planck-Institut für Biophysikalische Chemie, Postfach 2841, D-37018 Göttingen, Germany

(Received 25 June 1996; accepted 6 August 1996)

In previous papers the determination of the molecular contents of critical clusters has been performed. Both unary and binary vapor mixtures have been examined. This paper describes the first study of a ternary system. Using a nucleation pulse chamber accurate measurements of homogeneous nucleation rates ($10^5 < J/\mathrm{cm}^{-3}\,\mathrm{s}^{-1} < 10^9$) of mixed droplets in supersaturated, ternary mixtures of water, *n*-nonane and *n*-butanol vapor have been performed. The examined gas phase activities, a_1, a_2, and a_3, respectively, covered the whole ternary composition space at $T=240$ K. The observed variations of the cluster compositions with vapor phase composition differ substantially from that of ideal mixtures. The experiments seem to indicate phase separation within the critical clusters. The arrangement of the molecules in the cluster remains to be clarified. [S0021-9606(96)51642-9]

I. INTRODUCTION

In atmospheric as well as technological settings multicomponent condensation occurs. In technical processes often mixtures are encountered which form two or more condensed phases. For instance, in the liquid state water and oil do not mix. By adding a suitable third component, a surfactant, one achieves mixing. In emulsion and microemulsion research such systems are of growing importance. In the vapor phase there are no limitations to mutual mixing. For example, water and oil vapor form a homogeneous vapor phase. If such a vapor mixture is supersaturated, e.g., by an adiabatic expansion, water and oil droplets will form by homogeneous nucleation. Interestingly, water and oil nucleate independently.[1] Adding a third component the situation may change.

The seemingly difficult task to study *ternary* nucleation can be performed using a nucleation pulse expansion chamber.[2] The idea of a nucleation pulse is to generate supersaturation for a short period of time (of order of a millisecond). Only during that period nucleation occurs. By condensational growth the nuclei are then developed into droplets, the number density of which can then be determined by some optical technique. The knowledge of the time interval of nucleation and the number density of nuclei permits calculating a nucleation rate. As mentioned above, in the vapor phase one can mix any number of components. Therefore, also systems forming immiscible liquids can be studied.

Theoretical work of Kashchiev[3] predicts that isothermal nucleation rates versus supersaturation curves allow determining the number of molecules in the critical cluster. Using a nucleation pulse chamber we have constructed over the last years[2,4] investigations on the binary homogeneous nucleation of a variety of partially miscible liquid pairs have been performed.[1,5–8] In particular, water-*n*-alcohols at $T=260$ K[5,8] and water–nonane at $T=230$ K have been reported.[1] Presently we are studying the binary *n*-nonane–*n*-alcohol systems. In recent papers[6–8] we have extracted from nucleation rate measurements the molecular content of nuclei in binary systems. In the theoretical section we recall the theoretical procedure[6] and extend it to ternary systems. From the analysis of the measurements we obtain the composition of nuclei in some cases containing all three components. Towards the end of the paper we discuss how the molecules might be distributed.

II. THEORY

As Kashchiev[3] pointed out, the number of molecules in critical clusters is obtained from the steep dependence of nucleation rates on supersaturation without having to assume anything about the distribution of the matter within the cluster. While he suggested this first for unary systems, we later generalized it for binary systems.[6] Recently, Oxtoby, and Kashchiev[9] showed that

$$\left.\frac{\partial \Delta G^*}{\partial \Delta \mu_i}\right|_{\mu_k, k\neq i} = -n_i^*, \tag{1}$$

valid for any number of components, where the * refers to the critical cluster. ΔG^* is the work of formation of the critical cluster, and $\Delta\mu_i$ the chemical potential difference of molecule i in the vapor and condensed phase. Obtaining the numbers of molecules n_i^* in the nucleus independent of a particular model is useful for formulating and testing improved nucleation theories.

A. Nucleation theory

Generally, experimental nucleation rates follow the relation

$$J = K \exp\left(-\frac{\Delta G^*}{kT}\right), \tag{2}$$

[a]Present address: Finnish Meteorological Institute, Sahaajankatu 20E, SF-00810 Helsinki, Finland.
[b]Author to whom correspondence should be addressed.

which allows, in view of Eq. (1), to obtain the number of molecules in the critical cluster from

$$\left.\frac{\partial \ln J}{\partial \ln a_i}\right|_{a_k,k\neq i} \cong n_i^*, \tag{3}$$

because the kinetic prefactor K is a comparatively weak function of vapor phase activity a_i, which is taken as the ratio of the actual vapor pressure divided by the equilibrium vapor pressure of the pure component i.

B. Unary nucleation

The application of Eq. (3) to the case of nucleation of a single component has been demonstrated recently for a number of systems.[2,10,11] The activity for one component systems is usually called the supersaturation S. The number of molecules in the critical cluster are then obtained from the slope of the isothermal nucleation rate *curve*

$$\frac{d \ln J}{d \ln S} \cong n^*. \tag{4}$$

Interestingly, the molecular content of unary nuclei calculated from the Gibbs–Thomson equation using macroscopic surface tension and density agreed very well with the experimental n^* values.[2]

C. Binary nucleation

As it has been explained in detail by Strey and Viisanen[6] in 1993, from the experiments on binary systems a nucleation rate *surface* is obtained. The quantitative analysis of the slopes of this surface permits determining the individual numbers of both species in the binary nuclei. To recall the arguments, consider the nucleation rate surface $\ln J = f(a_1,a_2)$. At constant f, that is fixing $\ln J = \ln J_0$, where J_0 denotes a reference or onset nucleation rate, we have a onset activity line on the 2-dimensional $f(a_1,a_2)$ surface, so that

$$0 = \left.\frac{\partial f}{\partial a_1}\right|_{a_2} + \left.\frac{\partial f}{\partial a_2}\right|_{a_1} \left.\frac{\partial a_2}{\partial a_1}\right|_f. \tag{5}$$

Experimentally, one obtains $f(a,b)$ with

$$a = \sqrt{a_1^2 + a_2^2} \tag{6}$$

and a constant ratio b

$$b = \frac{a_2}{a_1}. \tag{7}$$

For any point on the surface we may write

$$\left.\frac{\partial f}{\partial a}\right|_b = \left.\frac{\partial f}{\partial a_1}\right|_{a_2} \left.\frac{\partial a_1}{\partial a}\right|_b + \left.\frac{\partial f}{\partial a_2}\right|_{a_1} \left.\frac{\partial a_2}{\partial a}\right|_b \tag{8}$$

with

$$\left.\frac{\partial a_1}{\partial a}\right|_b = \frac{1}{\sqrt{1+b^2}}, \tag{9}$$

$$\left.\frac{\partial a_2}{\partial a}\right|_b = \frac{b}{\sqrt{1+b^2}}. \tag{10}$$

Inserting Eq. (5) into Eq. (8) and rearranging, we find

$$\left.\frac{\partial f}{\partial a_2}\right|_{a_1} = \left.\frac{\partial f}{\partial a}\right|_b \left[\left.\frac{\partial a_2}{\partial a}\right|_b - \left.\frac{\partial a_2}{\partial a_1}\right|_f \left.\frac{\partial a_1}{\partial a}\right|_b\right]^{-1}, \tag{11}$$

$$\left.\frac{\partial f}{\partial a_1}\right|_{a_2} = -\left.\frac{\partial f}{\partial a_2}\right|_{a_1} \left.\frac{\partial a_2}{\partial a_1}\right|_f. \tag{12}$$

Inserting further Eqs. (9), (10), and (7) we can calculate $a_i \partial f/\partial a_i$ $(i=1,2)$, which is the desired $\partial \ln J/\partial \ln a_i \approx n_i^*$. This is because we could relate $\partial f/\partial a_i$ to the experimentally accessible quantities $\partial \ln J/\partial a|_b$, $b = a_2/a_1$ and $\partial a_2/\partial a_1|_J$. We note that Eqs. (11) and (12) are equivalent to Eqs. (35) and (36) of Strey and Viisanen[6] derived somewhat differently.

D. Ternary nucleation

In a ternary system one has three binary side systems. The experimental nucleation rate curves in each of the three binary systems shape nucleation rate surfaces in the *three*-dimensional J-a_1-a_2, J-a_1-a_3, and J-a_2-a_3 spaces, from which *lines* of onset activities are obtained. Emanating from the three binary sides, in *four*-dimensional J-a_1-a_2-a_3 space a nucleation rate hypersurface is formed, from which a *surface* of onset activities is obtained. Such a surface for the present system has experimentally been determined and is shown below. The individual numbers of the molecules in the nuclei can directly be determined from the slopes of the experimental nucleation rate hypersurface. In the case of ternary nucleation the problem arises that one seeks the nucleation rate as function of the activity of one component at a time, while keeping the other two activities constant. This is experimentally not feasible. Nevertheless, an analogous procedure as for binary nucleation is possible. Consider the nucleation rate *hypersurface* $\ln J = f(a_1,a_2,a_3)$ At constant f, that is $\ln J = \ln J_0$ we have an onset activity surface in 3-dimensional a_1-a_2-a_3 space, so that

$$0 = \left.\frac{\partial f}{\partial a_1}\right|_{a_2,a_3} + \left.\frac{\partial f}{\partial a_3}\right|_{a_1,a_2} \left.\frac{\partial a_3}{\partial a_1}\right|_{a_2,f}, \tag{13}$$

$$0 = \left.\frac{\partial f}{\partial a_2}\right|_{a_1,a_3} + \left.\frac{\partial f}{\partial a_3}\right|_{a_1,a_2} \left.\frac{\partial a_3}{\partial a_2}\right|_{a_1,f}. \tag{14}$$

Experimentally, we measure $f(a,b,c)$ with

$$a = \sqrt{a_1^2 + a_2^2 + a_3^2}, \tag{15}$$

$$b = \frac{a_2}{a_1}, \tag{16}$$

$$c = \frac{a_3}{a_1}, \tag{17}$$

which permit us to write in analogy with Eq. (8) for any point on the hypersurface

$$\left.\frac{\partial f}{\partial a}\right|_{b,c}=\left.\frac{\partial f}{\partial a_1}\right|_{a_2,a_3}\left.\frac{\partial a_1}{\partial a}\right|_{b,c}+\left.\frac{\partial f}{\partial a_2}\right|_{a_1,a_3}\left.\frac{\partial a_2}{\partial a}\right|_{b,c}+\left.\frac{\partial f}{\partial a_3}\right|_{a_1,a_2}\left.\frac{\partial a_3}{\partial a}\right|_{b,c}, \tag{18}$$

with

$$\left.\frac{\partial a_1}{\partial a}\right|_{b,c}=\frac{1}{\sqrt{1+b^2+c^2}}, \tag{19}$$

$$\left.\frac{\partial a_2}{\partial a}\right|_{b,c}=\frac{b}{\sqrt{1+b^2+c^2}}, \tag{20}$$

$$\left.\frac{\partial a_3}{\partial a}\right|_{b,c}=\frac{c}{\sqrt{1+b^2+c^2}}. \tag{21}$$

Inserting Eqs. (13) and (14) into Eq. (18) and rearranging we have

$$\left.\frac{\partial f}{\partial a_3}\right|_{a_1,a_2}=\left.\frac{\partial f}{\partial a}\right|_{b,c}\left[\left.\frac{\partial a_3}{\partial a}\right|_{b,c}-\left.\frac{\partial a_3}{\partial a_1}\right|_{f,a_2}\left.\frac{\partial a_1}{\partial a}\right|_{b,c}-\left.\frac{\partial a_3}{\partial a_2}\right|_{f,a_1}\left.\frac{\partial a_2}{\partial a}\right|_{b,c}\right]^{-1}. \tag{22}$$

The task is thus to determine $\partial \ln J/\partial a|_{b,c}$ and the orthogonal slopes $\partial a_3/\partial a_1|_{a_2,J}$ and $\partial a_3/\partial a_2|_{a_1,J}$ of the onset activity surface. Equation (22) can then be used in Eqs. (13) and (14)

$$\left.\frac{\partial f}{\partial a_2}\right|_{a_1,a_3}=-\left.\frac{\partial f}{\partial a_3}\right|_{a_1,a_2}\left.\frac{\partial a_3}{\partial a_2}\right|_{a_1,f}, \tag{23}$$

$$\left.\frac{\partial f}{\partial a_1}\right|_{a_2,a_3}=-\left.\frac{\partial f}{\partial a_3}\right|_{a_1,a_2}\left.\frac{\partial a_3}{\partial a_1}\right|_{a_2,f} \tag{24}$$

to obtain the other two slopes.

III. EXPERIMENT

A. Choice of the substances

The nucleation behavior of the unary system water[10] has been studied in our chamber before. *N*-nonane is an often studied nonpolar substance in homogeneous nucleation research.[4,12,13] With water and oil, two immiscible substances, as third substance the choice of an amphiphile seems to be interesting, because an amphiphile may link water and oil due to its molecular build up. Alcohols are simple amphiphiles, and the nucleation behavior of the *n*-alcohols is also well studied.[11,14,15] The choice of the alcohol for the present study rests on the following considerations. In general, the miscibility between water and an oil can be enhanced by the addition of a suitable amphiphile, but it is strongly temperature dependent.[16–18] From systematic investigations of the phase behavior water, oil amphiphile systems it is known that the efficiency of an amphiphile is most expressed at the so-called hydrophilic–lipophilic balance. There the interfacial tension between water and oil (of order 50 mN/m) are drastically reduced to a very low level (of order of 0.1 mN/m or less) by the presence of the amphiphile. As can be estimated from data given in the quoted papers[16–18] a balanced amphiphile at $T=240$ K for nonane as oil is *n*-butanol. Fixing the nucleation temperature to $T=240$ K is suggested by considering the experimental window for *n*-nonane. Homogeneously nucleated *n*-nonane droplets grow rather rapidly at higher temperatures than $T=240$ K,[4] while the nucleation of water[10] and *n*-butanol[11] can still well be studied.

B. The nucleation pulse experiment

The homogeneous nucleation rate measurements were performed using the nucleation pulse expansion chamber.[2] The vapors are premixed with the carrier gas in a separate receptacle from where a gas volume of selectable total pressure is filled into the chamber. For studying three components a third vaporizer was added to our vapor mixing unit. The three vapors water (1), *n*-nonane (2) and *n*-butanol (3) are admitted one at a time to the receptacle and the carrier gas (usually argon) is added in excess. After the vapors and the carrier gas have mixed in the receptacle the expansion chamber is flushed and filled with the vapor/carrier gas mixture. The details of the expansion chamber, experimental setup and the experimental procedure can be found in the quoted reference.[2] The total pressure and the pressure in the expansion volume are adjusted such that the subsequent expansion always leads to the same temperature ($T=240$ K) calculated by adiabatic law. Since the total pressure is recorded as function of time over the nucleation pulse the partial pressures p_1, p_2, and p_3 at nucleation temperature are precisely known. Using the known equilibrium partial pressures p_{10}, p_{20}, and p_{30} of the pure components the activities a_1, a_2, and a_3 are calculated. The expanded state is maintained for about 1 ms during which nucleation can occur. Then a small recompression is carried out to quench the nucleation process. In this fashion nuclei formed during the nucleation pulse can still grow and develop into droplets of micrometer size, where their number density C is determined by light scattering. Typical scattering curves are contained in previous publications.[2,4,10] Assuming the nucleation process to be stationary the nucleation rate is given by

$$J_{\exp}=\frac{C_{\exp}}{\Delta t_{\exp}}. \tag{25}$$

C. Accuracy of the results

The sources of experimental errors have been discussed by previously.[2,6] The experimental error of the nucleation rate J is estimated to be a factor of 2. The temperature calculated is accurate to within a few tenth of a degree and scatters less than a tenth of a degree. The slopes of the nucleation rates have a reproducibility of 4%. The determination of the onset activities leading to Fig. 1 is rather accurate, because they are supported by a whole nucleation rate curve. They carry an error of less than 3%. Connecting the a_3 vs a_{12} data points one obtains polygones. Determining the slopes

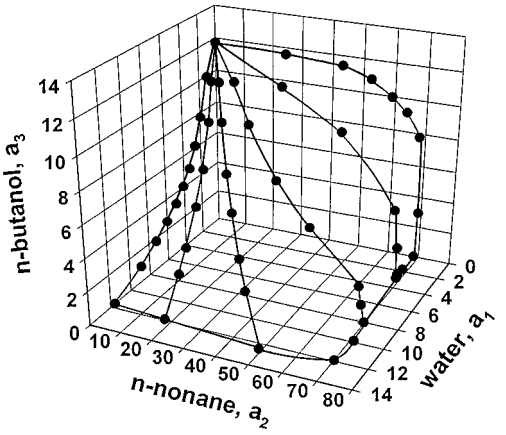

FIG. 1. The data points $a_3(a_1,a_2)$ in a_1-a_2-a_3 space (referring to a constant nucleation rate $J_0=10^7$ cm^{-3} s^{-1}) are shown in a 3-dimensional representation. The data are measured along lines of constant $b=a_2/a_1$ ratios by varying the *n*-butanol content. Full lines are aids to guide the eye. Each data point is obtained from a full nucleation rate curve. The data shape the onset activity surface discussed in the text.

for each a_3 data point introduces some error. Also the interpolation to obtain the a_2 vs a_1 curves has a similar uncertainty. Both slopes appear in a multiplicative fashion in Eqs. (29) and (30). Overall, we estimate the error in the x_i to be smaller than ± 0.05. The definitions of the quantities x_i and a_{12} follow below.

IV. RESULTS

A. The nucleation rate hypersurface

The experiment yields the nucleation rate J as function of the vapor phase activities a_1, a_2, and a_3. Since the vapors are mixed in the receptacle, the ratios b and c between the three activities stay constant as the total pressure is changed. Therefore, one may combine them into the single variable a defined above in Eq. (15). The $\ln J-a$ curves determine a nucleation rate *surface* in the $\ln J-a_i-a_j$ spaces of the *binary* systems. For discussion and a picture of a schematic nucleation rate surface see Ref. 6. For the *ternary* system studied here, the three binary nucleation rate surfaces bound a nucleation rate *hypersurface*, which is difficult to visualize in 3 dimensions. But we do not have to actually see the hypersurface, because it suffices to determine the slopes of that surface. Experimentally, measuring $\ln J-a$ curves for the ternary water–*n*-nonane–*n*-butanol system at constant temperature (240 K) is no more difficult than for a binary system. As for the binary systems the $\ln J-a$ representation of the datapoints is quite linear, so that least squares fits of straight lines to the data provide the numerical values for the slopes $\partial \ln J/\partial a|_{b,c}$ and the corresponding onset activities a_i. As mentioned, the $\ln J-a$ curves shape a hypersurface in the four-dimensional $\ln J$-a_1-a_2-a_3 space. Formally, this hypersurface may be thought to intersect with an a_1,-a_2,-a_3 hyperplane, if one fixes an onset nucleation rate at $J_0=10^7$ cm^{-3} s^{-1}, which represents the center of our experimental nucleation rate window, and is therefore rather precisely known. This is fully analogous to the binary system[6] where in 3-dimensional $\ln J$-a_1-a_2 space a nucleation rate surface intersects with an a_1-a_2 plane of constant onset nucleation rate of $J_0=10^7$ cm^{-3} s^{-1} to yield an a_1-a_2 line (the conventional activity plot in binary nucleation).

B. The onset activity surface

Accordingly, the intersection between the nucleation rate hypersurface and the a_1-a_2-a_3 hyperplane results in a surface in three-dimensional a_1-a_2-a_3 space. This surface we have determined experimentally. The $a_3(a_1,a_2)$ data points shaping the onset activity surface in a_1-a_2-a_3 space (referring to a constant $J=J_0$) are shown in Fig. 1 in a 3-dimensional representation. Due to the experimental procedure of fixing the $b=a_2/a_1$ ratio and changing the *n*-butanol content the data points in Fig. 1 follow smooth a_3 vs a_{12} curves, where we define

$$a_{12}=\sqrt{a_1^2+a_2^2}, \tag{26}$$

from which the slope $\partial a_3/\partial a_{12}|_b$ is obtained. Using the interpolations the between the $a_3(a_{12})$ data points for a given a_3 of interest a a_1-a_2 curve is constructed (lines of equal ''altitude'' so to speak, each containing six data points, one for each b-ratio investigated). Although we have not drawn these curves into Fig. 1 for clarity, it is conceivable that the a_1-a_2 curves permit determining the slope $\partial a_2/\partial a_1|_{a_3}$ for each $a_3(a_1,a_2)$ data point shown in Fig. 1. Since

$$\left.\frac{\partial a_1}{\partial a_{12}}\right|_b=\frac{1}{\sqrt{1+b^2}} \tag{27}$$

and

$$\left.\frac{\partial a_2}{\partial a_{12}}\right|_b=\frac{b}{\sqrt{1+b^2}}, \tag{28}$$

we have from Eqs. (11) and (12) [applied here to the $a_3(a_1,a_2)$ surface]

$$\left.\frac{\partial a_3}{\partial a_2}\right|_{a_1}=\left.\frac{\partial a_3}{\partial a_{12}}\right|_b\left[\frac{b}{\sqrt{1+b^2}}-\left.\frac{\partial a_2}{\partial a_1}\right|_{a_3}\frac{1}{\sqrt{1+b^2}}\right]^{-1}, \tag{29}$$

$$\left.\frac{\partial a_3}{\partial a_1}\right|_{a_2}=-\left.\frac{\partial a_3}{\partial a_2}\right|_{a_1}\left.\frac{\partial a_2}{\partial a_1}\right|_{a_3}. \tag{30}$$

As is seen from Eqs. (22) to (24) in the theoretical section in order to determine the number of molecules of each component in the critical nucleus, one needs (i) the slopes of the $\ln J-a$ curves (obtained directly from the experimental nucleation rate J versus a), ii) the orthogonal slopes $\partial a_3/\partial a_1|_{a_2}$ and $\partial a_3/\partial a_2|_{a_1}$ of the $a_3(a_1,a_2)$ surface [calculated from Eqs. (29) and (30) using the $\partial a_3/\partial a_{12}|_b$ and $\partial a_2/\partial a_1|_{a_3}$ obtained from the experimental surface as described].

TABLE I. For each experimental nucleation rate curve the slope $d \ln J/da|_T$ and the onset activities a_i are given. The numbers n_i of molecules in the clusters are obtained from the theoretical analysis of the nucleation rate hypersurface. Note that the negative numbers which occur are due the finite experimental error.

$d \ln J/da$	a_1	a_2	a_3	n_1	n_2	n_3
2.6435	11.614	0	0	30.7	0	0
3.1502	8.8773	0	0.9596	22.3	0	5.9
4.1072	7.2303	0	1.8011	20.9	0	9.7
4.4848	5.9657	0	2.5145	17.5	0	11.5
4.9490	4.9413	0	3.2622	16.2	0	13.1
5.3886	4.0899	0	4.0453	15.8	0	15.2
5.0263	3.3291	0	4.9134	14.6	0	15.3
4.5782	2.6234	0	6.1102	14.0	0	16.4
4.5193	1.9352	0	7.6921	13.9	0	22.0
3.9520	1.1016	0	9.9267	7.4	0	32.1
3.3551	0	0	11.724	0	0	39.3
1.3645	11.923	17.735	0	30.0	−0.8	0
1.6843	8.9495	13.223	1.0310	21.2	−0.5	6.2
2.2278	7.3126	10.631	1.8340	20.4	−0.2	8.8
3.1164	5.0111	7.2856	3.3414	16.3	−0.2	13.4
4.1573	3.3254	4.8638	5.0208	15.1	−0.0	17.1
4.1124	1.8978	2.7884	7.4401	11.5	0.2	21.9
3.8848	1.0903	1.5828	9.6811	7.5	0.3	30.6
3.3551	0	0	11.724	0	0	39.4
0.5486	12.464	48.933	0	27.7	0.0	0
0.7965	9.2525	35.902	1.0705	20.7	1.6	7.3
1.0413	7.3386	28.665	1.8486	21.9	−0.8	9.7
1.4080	5.0076	19.532	3.3686	16.2	−0.8	13.4
2.2193	3.3129	12.903	4.9865	15.6	−0.7	16.7
3.0882	1.8782	7.3452	7.5527	11.9	−0.5	21.6
3.4456	1.0788	4.2130	9.6933	7.6	−0.4	29.4
3.3551	0	0	11.724	0	0	39.4
0.3260	8.0071	69.742	0	−.9	23.8	0
0.3065	7.8130	68.415	0.8899	7.4	13.4	0.3
0.4254	7.7784	67.515	1.9547	11.9	10.8	5.6
0.6832	5.2525	46.030	3.5218	12.5	4.4	14.9
1.0186	3.4353	30.209	5.1966	13.2	1.1	17.1
1.8124	1.9251	16.900	7.7189	12.1	−0.8	22.6
2.9224	1.1168	9.6871	9.8846	8.3	−0.6	32.9
3.3551	0	0	11.724	0	0	39.3
0.3223	2.8822	68.670	0	−0.2	22.3	0
0.2507	2.9136	69.073	0.3071	−0.1	17.6	−0.2
0.3221	3.0447	70.961	0.7566	0.0	22.8	0.1
0.2995	2.8951	68.620	1.9788	0.2	19.8	0.6
0.2717	2.8718	67.291	4.3338	3.5	11.6	3.2
0.6877	2.0458	47.965	8.2667	8.4	6.5	18.6
1.3161	1.1027	25.981	10.044	3.9	1.8	30.9
3.3551	0	0	11.724	0	0	39.3
0.3297	0	68.365	0	0	22.5	0
0.3705	0	69.152	2.9452	0	25.6	0.0
0.3453	0	68.146	7.7952	0	21.6	2.1
0.4253	0	63.901	9.1895	0	17.2	10.3
0.3681	0	59.100	9.9766	0	10.1	11.9
0.4215	0	52.423	10.834	0	6.8	15.7
0.6722	0	43.194	11.407	0	2.8	27.3
1.2589	0	24.330	11.589	0	0.5	33.4
3.3551	0	0	11.724	0	0	39.3
2.6435	11.614	0	0	30.7	0	0
1.3645	11.923	17.735	0	30.0	−0.8	0
0.5486	12.464	48.933	0	27.7	0.0	0
0.3354	11.917	70.084	0	14.1	9.7	0
0.3274	9.8773	71.022	0	−0.3	23.8	0
0.3260	8.0071	69.742	0	−0.9	23.8	0
0.3223	2.8822	68.670	0	−0.2	22.3	0
0.3297	0	68.365	0	0	22.5	0

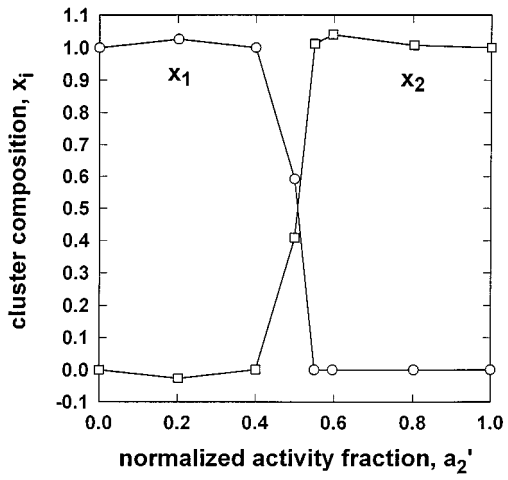

FIG. 2. The composition of the clusters in the binary water–*n*-nonane systems versus the normalized onset activities. As can be seen either water or oil droplets nucleate abruptly changing from one type to the other at $a_2' = 0.5$. Note that the negative numbers are within experimental error equal to zero, numbers larger than unity are within experimental error equal to unity.

C. Measurement of molecular content of the nuclei

The n_1, n_2, and n_3, that are the measured numbers of water, *n*-nonane and *n*-butanol molecules for each data point in Fig. 1 have been determined and are given in Table I. In Table I we give the slope of the nucleation rate curve, the a_i and the n_i with more than significant digits in order for the reader to be able perform calculations without limiting rounding errors. The actual numbers for the one-component systems are for water 31, for *n*-nonane 23, and for *n*-butanol 39 molecules in the critical clusters. The numbers of molecules of the binary and ternary systems vary smoothly within these limits and are most instructively plotted by calculating the mole fractions

$$x_i = n_i \Big/ \sum_i n_i \quad (i=1,2,3). \tag{31}$$

In Fig. 2 the composition of the clusters in the binary water–*n*-nonane systems are shown. The excursions of the data points x_i to values $x_i<0$ and >1 are within experimental error consistent with being $x_i=0$ or $=1$, respectively. The normalization of the abscissa by the onset activities a_{i0} $(i=1,2)$ of the respective pure systems permits representing the data evenly spaced. We therefore define a normalized activity fraction

$$a_2' \equiv \frac{a_2/a_{20}}{a_1/a_{10}+a_2/a_{20}}. \tag{32}$$

As can be seen either water or oil droplets nucleate. At $a_2' = 0.5$ the nucleating species abruptly switches from water to oil. This behavior is consistent with the direct observation considering the bottom plane of Fig. 1, where the onset activity for nucleation is observed to be either that of water or oil.

In Figs. 3(a)–3(f) the full ternary system is presented ranging from the pure binary water–*n*-butanol system (a_2'

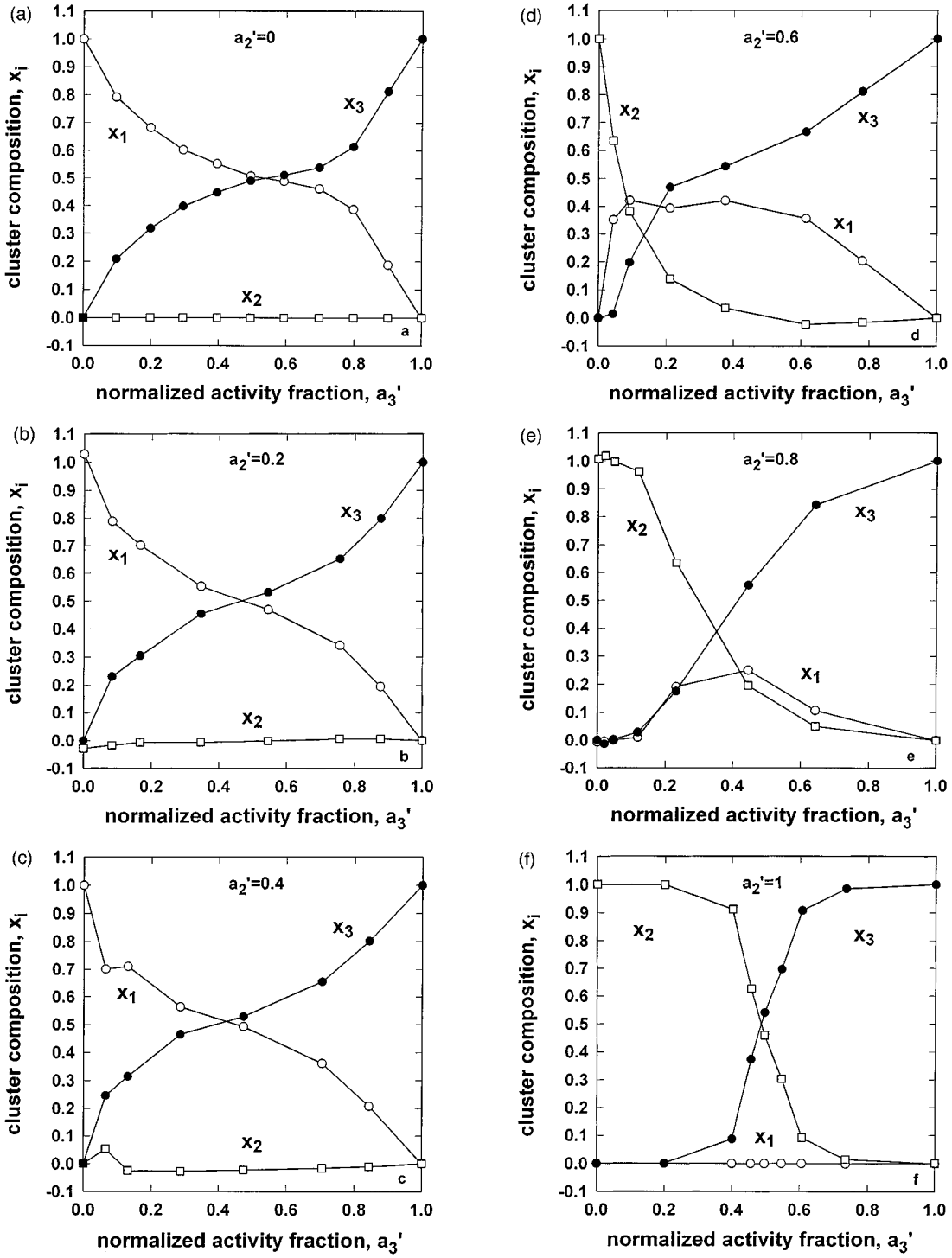

FIG. 3. Compositions of the ternary cluster versus the normalized activity fraction of *n*-butanol a_3'. (a) pure water–*n*-butanol, $a_2' = 0$, (b) $a_2' = 0.2$, (c) $a_2' = 0.4$, (d) $a_2' = 0.6$, (e) $a_2' = 0.8$, (f) $a_2' = 1$. Note that at intermediate a_2' all three components are simultaneously nucleating in significant amounts. The error in x_i is smaller than ± 0.05. For the individual numbers of molecules refer to Table I.

$= 0$) to the pure binary *n*-butanol–*n*-nonane system ($a_2' = 1$). Here, the data are plotted versus the normalized activity fraction of *n*-butanol, where we define

$$a_3' \equiv \frac{a_3/a_{30}}{a_1/a_{10} + a_2/a_{20} + a_3/a_{30}}. \tag{33}$$

Considering once more Fig. 1, each of the plots in Fig. 3 starts at a point on the bottom plane in Fig. 1 (for a given a_2' ratio ranging from 0 to 1) and a_3' increases until one ends up at the pure butanol corner where a_3' is unity, *per definitionem*. Let us consider the individual plots one by one. Starting in Fig. 3(a) with pure water–*n*-butanol ($a_2' = 0$), one

can see that water nucleates at low a_3'. Also it can be seen that *n*-butanol enhances water nucleation and vice versa, so that at intermediate vapor compositions the cluster compositions are quite similar. For $a_2' = 0.2$ in Fig. 3(b) not much has changed. We note that in the evaluation procedure the number of oil molecules are measured to be effectively zero. Remarkably, within experimental error no oil molecules participates in the nucleation process. Negative numbers are of course the consequence of the finite experimental accuracy. For $a_2' = 0.4$ in Fig. 3(c) there is again not much change, except for the little glitch of the x_2 which may in fact a precursor of what happens for the next higher a_2' in Fig. 3(d). Here, for $a_2' = 0.6$, the situation has qualitatively changed: the nucleation starts with pure *n*-nonane, so that $x_2=1$ for $a_3=0$. However, as soon as some *n*-butanol is present in the critical cluster a rapid entering of water is observed while *n*-nonane becomes less. In Fig. 3(e), for $a_2' = 0.8$, the situation is qualitatively similar although quantitatively now *n*-nonane and butanol dominate. However, at some intermediate normalized activity, e.g., $a_3' = 0.35$, all three components are found to be simultaneously present in significant amounts. The binary *n*-nonane–*n*-butanol system ($a_2' = 1$) in Fig. 3(f) displays a rather reluctant conucleation of *n*-nonane and butanol. If one looks back to Fig. 1 this behavior is already visible in the onset activity surface, where in binary *n*-nonane–*n*-butanol system rather high activities are required at intermediate vapor compositions.

For vapor mixtures of three components we have found cluster compositions with significant amounts of all three components. Thus, it seems that the amphiphile, *n*-butanol, does work as a surfactant: It links the two incompatible components water and *n*-nonane in a single cluster, which is a typical feature of surfactants. Whether it does this in form of a molecular mixture or in the form of two or more phases remains to be found out. In previous papers evidence of surface enrichment of alcohol in binary water–*n*-alcohol systems was found. If in addition oil enters the cluster it will (presumably) seek contact with the hydrophobic part and avoid contact with the water-rich core. That is, phase separation within the cluster is likely to occur. Here, the question of definition of a phase consisting of a few molecules arises. Also, phase separated critical clusters require theoretical models for the structure of such clusters. Progress could come from techniques, like molecular dynamics,[19] Monte Carlo, and and density functional theory.[20,21] In the quoted work phase separated clusters have been investigated and their structure analyzed. Experiments of the type described in this paper furnish quantitative data (cf. Table I) on the actual number of molecules within the cluster.

V. CONCLUSIONS

We have demonstrated how simultaneous nucleation of three components can experimentally be examined. Furthermore, we have given the mathematical treatment of the experimental measurables from which we extracted the individual numbers of molecules, that is, the cluster composition. The procedure, as described, can be applied to any kind of ternary mixture. Specifically, one might think of atmospherically relevant mixtures of water and trace gases. Experiments on such systems are planned for the future. We have studied here the condensation of the immiscible pair water–*n*-nonane and examined how the addition of an amphiphile links the two incompatible liquids in a cluster. It is remarkable that at intermediate vapor compositions the critical clusters contain significant amounts of each component. The quantitative numbers we have determined may constitute a basis for theoretical modeling of the (presumably) inhomogeous distribution of the molecules in such clusters.

ACKNOWLEDGMENTS

The present work was performed in the department of Professor M. Kahlweit to whom we are indebted for support. We, furthermore, acknowledge a continuing cooperation with Professor P. E. Wagner.

[1] P. E. Wagner and R. Strey, *Aerosols in Science, Industry and Environment* (Proceedings of the 3rd International Aerosol Conference, Kyoto 1990) edited by S. Masuda and K. Takahashi (Pergamon, Oxford, (1990), p. 201.
[2] R. Strey, P. E. Wagner, and Y. Viisanen, J. Phys. Chem. **98**, 7748 (1994).
[3] D. Kashchiev, J. Chem. Phys. **76**, 5098 (1982).
[4] P. E. Wagner and R. Strey, J. Chem. Phys. **80**, 5266 (1984).
[5] R. Strey and P. E. Wagner, in *Atmospheric Aerosols and Nucleation*, Lecture Notes in Physics, Vol. 309 (Springer, Berlin, 1988) p. 111.
[6] R. Strey and Y. Viisanen, J. Chem. Phys. **99**, 4693 (1993).
[7] Y. Viisanen, R. Strey, A. Laaksonen, and M. Kulmala, J. Chem. Phys. **100**, 6062 (1994).
[8] R. Strey, Y. Viisanen, and P. E. Wagner, J. Chem. Phys. **103**, 4333 (1995).
[9] D. W. Oxtoby and D. Kaschiev, J. Chem. Phys. **100**, 7665 (1994).
[10] Y. Viisanen, R. Strey, and H. Reiss, J. Chem. Phys. **99**, 4680 (1993).
[11] Y. Viisanen and R. Strey, J. Chem. Phys. **101**, 7835 (1994).
[12] C. Hung, M. J. Kransnopoler, and J. L. Katz, Chem. Phys. **90**, 1856 (1989).
[13] G. W. Adams, J. L. Schmitt, and R. A. Zalabsky, J. Chem. Phys. **81**, 5074 (1984).
[14] R. Strey, P. E. Wagner, and T. Schmeling, J. Chem. Phys. **84**, 2325 (1986).
[15] J. Hruby, Y. Viisanen, and R. Strey, J. Chem. Phys. **104**, 5181 (1996).
[16] M. Kahlweit and R. Strey, Angew. Chem. Int. Ed. **24**, 654 (1985).
[17] M. Kahlweit, R. Strey, and P. Firman, J. Phys. Chem. **90**, 671 (1986).
[18] R. Strey, Colloid Polymer Sci. **272**, 1005 (1994).
[19] A. S. Clarke, R. Kapral, B. Moore, G. Patey, and X.-G. Wu, Phys. Rev. Lett. **70**, 3283 (1993).
[20] A. Laaksonen and D. W. Oxtoby, J. Chem. Phys. **102**, 5803 (1995).
[21] V. Talanquer and D. W. Oxtoby, J. Chem. Phys. **104**, 1993 (1996).